Petroleum Science 21 (2024) 4189–4203

Contents lists available at ScienceDirect

Petroleum Science

journal homepage: www.keaipublishing.com/en/journals/petroleum-science

Original Paper

Feasibility of CO_2 storage and enhanced gas recovery in depleted tight sandstone gas reservoirs within multi-stage fracturing horizontal wells

Er-Meng Zhao [a, b], Zhi-Jun Jin [a, b, *], Gen-Sheng Li [c, b], Kai-Qiang Zhang [a, b], Yue Zeng [b]

[a] Institute of Energy, Peking University, Beijing, 100871, PR China
[b] Ordos Research Institute of Energy, Peking University, Ordos, 017010, Inner Mongolia, PR China
[c] State Key Laboratory of Petroleum Resources and Engineering, China University of Petroleum (Beijing), Beijing, 102249, PR China

ARTICLE INFO

Article history:
Received 4 June 2024
Received in revised form
22 August 2024
Accepted 31 August 2024
Available online 19 September 2024

Edited by Yan-Hua Sun

Keywords:
Tight sandstone gas reservoir
CO_2 geological storage
Enhanced gas recovery
Multi-stage fracturing horizontal well
Numerical simulation

ABSTRACT

Injecting CO_2 when the gas reservoir of tight sandstone is depleted can achieve the dual purposes of greenhouse gas storage and enhanced gas recovery (CS-EGR). To evaluate the feasibility of CO_2 injection to enhance gas recovery and understand the production mechanism, a numerical simulation model of CS-EGR in multi-stage fracturing horizontal wells is established. The behavior of gas production and CO_2 sequestration is then analyzed through numerical simulation, and the impact of fracture parameters on production performance is examined. Simulation results show that the production rate increases significantly and a large amount of CO_2 is stored in the reservoir, proving the technical potential. However, hydraulic fractures accelerate CO_2 breakthrough, resulting in lower gas recovery and lower CO_2 storage than in gas reservoirs without fracturing. Increasing the length of hydraulic fractures can significantly increase CH_4 production, but CO_2 breakthrough will advance. Staggered and spaced perforation of hydraulic fractures in injection wells and production wells changes the fluid flow path, which can delay CO_2 breakthrough and benefit production efficiency. The fracture network of massive hydraulic fracturing has a positive effect on the CS-EGR. As a result, CH_4 production, gas recovery, and CO_2 storage increase with the increase in stimulated reservoir volume.

1. Introduction

The greenhouse effect caused by massive CO_2 emissions during the industrialization process has a serious impact on the environment and has increasingly aroused public concern (Meinshausen et al., 2009; Yoro and Daramola, 2020). CO_2 capture and storage/CO_2 capture utilization and storage (CCS/CCUS) technology is considered a promising way to reduce CO_2 emissions and has received widespread attention from industry and academia (Wang Y.Y. et al., 2023). The targets for CO_2 geological storage mainly include saline aquifers (Li S. et al., 2023) depleted oil and gas reservoirs (Prasad et al., 2023; Sambo et al., 2023), unminable coal seams (Singh et al., 2023), and natural gas hydrate reservoirs (Zhang K. et al., 2022). The mechanisms of geological storage are summarized through experiments and numerical simulations as structural storage, dissolution storage, residual gas storage, mineralization storage, and adsorption storage (Davoodi et al., 2023; Zuo et al., 2023). Injecting CO_2 into depleted oil and gas reservoirs can improve oil and gas recovery while burying a large amount of CO_2 in the reservoir, which has significant economic and environmental benefits (Edouard et al., 2023). Compared with other geological targets, depleted gas reservoirs are more suitable for CO_2 storage because natural gas is more compressible than crude oil and the recovery of gas reservoirs is higher than that of oil reservoirs (Odi, 2012; Luo et al., 2023). In addition, the long-term occurrence of natural gas during the accumulation process has proven the superiority of gas reservoirs in preventing CO_2 leakage (Wang W. et al., 2023). At present, some CS-EGR field tests have been successfully implemented, such as the ORC project of the K12-B gas field in the North Sea of the Netherlands (Van der Meer et al., 2005), the Otway project in Australia (Underschultz et al., 2011), etc., which provide valuable experience for the large-scale application of CO_2 injection in depleted gas reservoirs.

* Corresponding author.
E-mail address: jinzj1957@pku.edu.cn (Z.-J. Jin).

https://doi.org/10.1016/j.petsci.2024.08.014

In recent years, many experiments and numerical simulations have been carried out focusing on enhanced gas recovery and CO_2 storage mechanisms, production dynamics analysis, storage potential and technical feasibility assessment, involving conventional sandstone gas reservoirs, coalbed methane reservoirs and shale gas reservoirs (Hamza et al., 2021; Liu et al., 2022a, 2022b; Shen et al., 2024). Ennis-King et al. (2011) and Luo et al. (2013) studied the impact of heterogeneity of the vertical permeability on the CS-EGR process based on numerical simulations. Their results showed that CO_2 preferentially breaks through from the high-permeability layer, which is not conducive to CH_4 production and CO_2 storage. The pores of gas reservoirs usually contain irreducible water, which inevitably affects gas production and CO_2 storage in the CS-EGR process. The numerical simulation results of Patel et al. (2017) showed that irreducible water changes the CO_2 flow field in the reservoir, thereby accelerating CO_2 breakthrough in production wells and reducing CH_4 recovery. However, He et al. (2023) found that as the irreducible water saturation increased from 0 to 40%, the CH_4 recovery increased by 4.37% and the cumulative CO_2 storage decreased by 21.24%. To accurately calculate the CO_2 storage capacity in depleted gas reservoirs, He et al. (2024) established an analytical model that considers CO_2 dissolution in formation water based on the molar balance principle. Research results show that CO_2 storage capacity is significantly improved after considering dissolution, and CO_2 dissolution cannot be ignored in gas reservoirs with high water saturation or edge and bottom water. In addition, many scholars have conducted research on the CO_2 flooding process of different types of gas reservoirs. Asif et al. (2024) developed a comprehensive method to analyze the binary adsorption balance, diffusion and dispersion in the process of CO_2 enhanced coal bed methane recovery (CO_2-ECBM). The results show that CO_2 exhibits higher adsorption capacity than CH_4, and the Langmuir volume of CO_2 is 2.0–2.3 times that of CH_4. Li Z. et al. (2023) established a fully coupled model for coal seam deformation, gas flow, and heat transfer, and conducted numerical simulations of CO_2-ECBM in the Qinshui Basin. It was found that increasing the injection temperature can significantly enhance the gas displacement process. Zhang et al. (2023) experimentally studied the synergistic effect of CH_4 recovery and CO_2 storage in the CO_2-ECBM process, showing that the implementation of CO_2-ECBM technology can increase the CH_4 recovery from 66.67% of conventional coalbed methane production technology to 90.86%–93.50%. Considering viscous flow, Knudsen diffusion, gas slip, component competitive adsorption, and real gas effects, Tang et al. (2023) established a dual medium multi-component flow model for shale gas reservoirs, and simulated the feasibility of CO_2 injection to enhance gas recovery and CO_2 sequestration. Their results revealed that the adsorption ratio of injected CO_2 in shale gas reservoirs is 45%–60%, and the CH_4 recovery is increased by 10%–15%. Gao et al. (2024) established a wellbore-reservoir-temperature-flow-mechanics-diffusion coupling mathematical model, and studied the changing characteristics of mass transfer, heat transfer and gas physical properties in the wellbore and reservoir during CO_2 injection in the gas reservoir.

The natural gas resources in tight sandstone are abundant and have enormous development potential. For example, in the Ordos Basin of China, the resource amount reaches 13.3×10^{12} m^3 (Yu et al., 2023). Compared with conventional medium-to-high permeability gas reservoirs, tight sandstone gas reservoirs generally exhibit poor reservoir physical properties and strong heterogeneity, resulting in low production and poor efficiency in vertical well development (Blasingame, 2008; Li et al., 2020). Horizontal well multi-stage hydraulic fracturing technology can significantly increase gas production and has become an effective way for efficient development of tight gas reservoirs, and has been widely applied in mining fields in recent years (He et al., 2014). However, due to the low formation pressure coefficient of gas reservoirs and rapid pressure decline during development, depressurization development relying on the natural energy of the reservoir shows the characteristics of rapid production decline (Guo et al., 2017). The main methods used to improve gas recovery include reducing abandoned pressure, pressurized mining, and increasing well network density (Wu et al., 2023). Nevertheless, the gas recovery is still below 50% when the gas reservoir is depleted (Zhang L. et al., 2022). At this time, injecting CO_2 into the depleted gas reservoir to supplement the formation pressure can achieve the dual goals of improving gas recovery and CO_2 storage. In addition, tight sandstone gas reservoirs have greater potential for enhanced gas recovery than conventional medium-to-high permeability gas reservoirs (Wang W. et al., 2023).

In recent years, extensive research has been conducted on CO_2 flooding of depleted tight sandstone gas reservoirs in terms of enhanced gas recovery and CO_2 storage potential, technical feasibility and production characteristics. Shi et al. (2017) conducted core experiments to evaluate the potential of CO_2 injection in tight gas reservoirs to enhance gas recovery, showing that when the CO_2 content at the core outlet is 10%, the CH_4 recovery can be increased by 12% compared with depletion development. The long core experimental results of Wang et al. (2018) showed that CO_2 flooding can increase gas recovery by 18.36% and CO_2 geological storage exceeds 60%, confirming the feasibility of CS-EGR technology in tight gas reservoirs. Based on experimental and simulation studies, Jia et al. (2019) summarized the mechanism of CO_2 injection to enhance gas recovery of tight gas reservoirs as the partial miscibility of CO_2 and natural gas, pressure maintenance and the cushioning effect of CO_2. The partial miscibility phenomenon between CO_2 and CH_4 in tight gas reservoirs has also been verified in other studies (Liao et al., 2023). Jia et al. (2021) conducted a numerical simulation study of CO_2 injection based on geological and production data from China's DND tight gas field, which showed that the gas recovery can be improved by 8.0%–9.5%. Ding et al. (2021) found that due to the higher density and viscosity of supercritical CO_2, injecting CO_2 into tight gas reservoirs can achieve near-piston displacement, which further confirms the feasibility. Long core experiments based on the tight sandstone of the Ordos Basin illustrated that supercritical CO_2 flooding increases the recovery by 18%–24% and the CO_2 storage rate is greater than 85% (Ding et al., 2021). Some scholars have conducted experimental studies of the factors affecting gas recovery and CO_2 storage, and found that the increase in CH_4 recovery decreases with the increase in permeability (Syah et al., 2021). For tight gas reservoirs with lower permeability, higher water saturation, and larger dip angles, it has a higher efficiency in improving recovery and storage capacity (Ding et al., 2022).

The above research results have confirmed that CS-EGR is a promising method for improving the gas recovery, extending production life, and reducing greenhouse gas emissions of tight sandstone gas reservoirs. In addition, the extensive application of multi-stage fracturing horizontal well in the development implies that these production wells will become the basic well pattern for CO_2 flooding after the tight gas reservoirs are depleted. Previous studies have discussed the influence of geological and engineering factors (permeability, heterogeneity, bound water saturation, injection–production well perforation location, injection rate, etc.) on the CO_2 flooding process in the vertical well pattern model. However, horizontal wells and hydraulic fractures in multi-stage fractured horizontal well pattern will change the fluid flow path, resulting in significant differences in CO_2 flooding behavior compared with the vertical well pattern. To our knowledge, the technical potential of CO_2 flooding for enhanced gas recovery and

CO_2 sequestration has not been well evaluated. Therefore, it is of great significance to evaluate the technical feasibility of CS-EGR under multi-stage fracturing horizontal well mode in tight sandstone gas reservoirs. Numerical simulation methods can provide details on CO_2 flooding characteristics and production dynamics at the reservoir scale, which will contribute to the success of field applications. In this work, based on the geological and engineering parameters of the Sulige Gas Field in the Ordos Basin, a numerical model for CO_2 flooding of multi-stage fracturing horizontal wells in depleted tight sandstone gas reservoirs is first established. Then the technical feasibility of CS-EGR is evaluated based on numerical simulation, and the dynamic behavior of gas production and CO_2 storage during the flooding process is analyzed. Finally, the effects of hydraulic fracture parameters on CH_4 production and CO_2 storage are comprehensively discussed. The research results can provide theoretical support and useful reference for the field application of CS-EGR engineering.

2. Mathematical model

The mathematical model considers the flow of gaseous and aqueous phases in porous media, the molecular diffusion of CO_2 and CH_4, and the dissolution of CO_2 in aqueous phase. The competitive adsorption between CH_4 and CO_2 in tight sandstone gas reservoirs during CO_2 flooding is ignored in this work.

The CH_4 component mainly exists in the gaseous phase, ignoring its dissolution in the aqueous phase. The mass conservation equation of CH_4 component can be expressed as follows:

$$\frac{\partial}{\partial t}\left(\phi S_G \rho_G X_G^m\right) + \nabla \cdot \left(X_G^m \boldsymbol{v}_G\right) + \nabla \cdot \boldsymbol{J}_G^m = X_G^m q_G \tag{1}$$

where t represents time, s; ϕ represents porosity; S_G represents gas saturation; ρ_G represents gaseous phase density, kg/m^3; X_G^m represents the mass fraction of CH_4 component in the gaseous phase; $\boldsymbol{v}_G$ represents the flow velocity vector of the gaseous phase, kg/m^2/s; $\boldsymbol{J}_G^m$ represents the diffusion rate of CH_4 component in the gaseous phase, kg/m^2/s; q_G represents the mass rate of gaseous phase per unit reservoir volume in the well, kg/m^3/s.

The CO_2 component exists in both gaseous and aqueous phases, and its mass conservation equation can be expressed as

$$\frac{\partial}{\partial t}\left(\sum_{\beta=A,G} \phi S_\beta \rho_\beta X_\beta^c\right) + \nabla \cdot \left(\sum_{\beta=A,G} X_\beta^c \boldsymbol{v}_\beta\right) + \nabla \cdot \boldsymbol{J}_\beta^c = \sum_{\beta=A,G} X_\beta^c q_\beta \tag{2}$$

where β represents the fluid phase, β = A, G represents aqueous phase and gaseous phase respectively; S_β represents the saturation of β phase; ρ_β represents the density of β phase, kg/m^3; X_β^c represents the mass fraction of CO_2 in the β phase; $\boldsymbol{v}_\beta$ represents the flow velocity vector of β phase, kg/m^2/s; $\boldsymbol{J}_\beta^c$ represents the diffusion rate of CO_2 component in β phase, kg/m^2/s; q_β represents the mass rate of β phase per unit reservoir volume in the well, kg/m^3/s.

The water component exists in both the aqueous and gaseous phases, and its mass conservation equation can be expressed as

$$\frac{\partial}{\partial t}\left(\sum_{\beta=A,G} \phi S_\beta \rho_\beta X_\beta^w\right) + \nabla \cdot \left(\sum_{\beta=A,G} X_\beta^w \boldsymbol{v}_\beta\right) = \sum_{\beta=A,G} X_\beta^w q_\beta \tag{3}$$

where X_β^w represents the mass fraction of water component in the β phase.

The fluid flow of gaseous and aqueous phases is assumed to follow Darcy's law, as follows:

$$\boldsymbol{v}_\beta = -K\frac{K_{r\beta}\rho_\beta}{\mu_\beta}\left(\nabla p_\beta - \rho_\beta \boldsymbol{g}\right) \tag{4}$$

where K represents permeability, m^2; $K_{r\beta}$ represents the relative permeability of the β phase; μ_β represents the viscosity of the β phase, Pa·s; p_β represents the pressure of the β phase, Pa; $\boldsymbol{g}$ represents the gravitational acceleration vector, m/s^2.

The diffusion mass rate of components in gas and water phases is calculated using the following formula:

$$\boldsymbol{J}_\beta^\kappa = -\frac{D_\beta^\kappa}{\tau_\beta}\phi S_\beta \rho_\beta \nabla X_\beta^\kappa \tag{5}$$

where D_β^κ represents the diffusion coefficient of the κ component in the β phase, m^2/s; τ_β represents the tortuosity of the reservoir.

The dissolution of CO_2 in aqueous phase is calculated based on Henry's law as follows:

$$f_{CO_2}^A = H_{CO_2} x_{CO_2}^A \tag{6}$$

where $f_{CO_2}^A$ represents the fugacity of CO_2 in aqueous phase, MPa; H_{CO_2} represents the Henry constant of CO_2, MPa; $x_{CO_2}^A$ represents the molar fraction of CO_2 in the aqueous phase.

The Henry constant changes with pressure, and the effect of pressure on the Henry constant can be calculated using the following equation:

$$\ln H_{CO_2} = \ln H_{CO_2}^{sat} + \frac{1}{RT}\int_{p_{H_2O}^{sat}}^{p_M} v_{CO_2}^\infty \, dp_M \tag{7}$$

where $H_{CO_2}^{sat}$ represents the Henry constant of CO_2 under water saturation pressure conditions in MPa, which can be calculated using the method in references Harvey (1996), Garcia (2001); Bakker (2003); R is the gas constant, J/mol/K; T is temperature, K; p_M represents the reservoir pressure, MPa; $p_{H_2O}^{sat}$ represents the vapor pressure of water under reservoir conditions, MPa; $v_{CO_2}^\infty$ represents the partial molar volume of CO_2 in an infinitely diluted aqueous solution, cm^3/mol.

In order to verify the accuracy of the mathematical model, the experimental results of CO_2 flooding in long cores of tight sandstone gas reservoirs have been compared with the numerical simulation results, as shown in our previous simulation work (Zhao et al., 2024). The comparison results show that there is a good agreement between the experimental and simulated data of CO_2 content in the output gas of the core in the whole process of CO_2 flooding. The results suggest that the mathematical model can effectively simulate the production dynamics of CO_2 flooding in depleted tight sandstone gas reservoirs.

3. Numerical simulation model

The Sulige Gas Field is located on the northwest side of the Yishan Slope in the Ordos Basin, with the main gas-bearing layers being the Upper Paleozoic Shihezi Formation and Shanxi Formation (Ji et al., 2019). As a typical tight sandstone gas field, it has the characteristics of low porosity, low permeability, low pressure, and low abundance (Wu et al., 2023). The average porosity of the reservoir is 4%–12%, the average permeability is 0.01–1 mD, and the pressure coefficient is 0.62–0.90 (Fu et al., 2019). Due to the close range migration and accumulation of CH_4, the saturation of bound water is usually high (Zhao et al., 2012). Multi-stage

hydraulic fracturing horizontal well technology can significantly improve reservoir seepage capacity, which is an effective way to increase the production of tight gas reservoirs. The Sulige Gas Field began exploring multi-stage fracturing horizontal well technology in 2008, and has successively gone through stages such as experimental breakthroughs, large-scale applications, and optimization and improvement. At present, the length of horizontal wells has increased from 843 to 1299 m, and the number of fracturing strips has increased from 3–5 sections to 8–10 sections, forming an overall development zone for horizontal wells in the southeast of Sulige (He et al., 2014; Wang et al., 2021). In our previous work, the feasibility of injecting CO_2 into tight gas reservoirs to enhance gas recovery under five-point well pattern through numerical simulation method (Zhao et al., 2024).

In this work, a numerical simulation model is established based on the typical geology and the engineering parameters of multi-stage fracturing horizontal wells in the southeastern Sulige area. The reservoir porosity is set to 0.077, and the horizontal and vertical permeabilities are 0.37×10^{-15} and 0.037×10^{-15} μm^2, respectively. The fluid in the gas reservoir is composed of gas phase and water phase. The gas saturation is 0.60, the irreducible water saturation is 0.40, and the residual gas saturation is 0.15. As shown in Fig. 1, the dimensions of the model in the x, y, and z directions are 1455 m × 1200 m × 30 m. Two parallel horizontal wells act as a CO_2 injection well and a production well, respectively, with a well spacing of 615 m and a horizontal well length of 1065 m. The grid size in the x and y directions is 15 m, and the grid size in the z direction is 2 m, thus a total of $97 \times 80 \times 15 = 116400$ grid cells are generated after discretization. Both horizontal wells are fractured into 8 hydraulic fractures, and it is assumed that each hydraulic fracture completely penetrated the gas layer. The hydraulic fracture spacing is 150 m, the fracture half-length is 150 m, and the fracture conductivity is 40 D·cm. The initial reservoir pressure of the gas reservoir is 28 MPa. When the gas reservoir is developed by consuming natural energy and reaches an average reservoir pressure of 8 MPa, the gas reservoir will be depleted due to too low production rate. Then one production well is converted into an injection well, and CO_2 is injected to displace CH_4 gas at a constant rate to enhance gas recovery, while the other production well maintains a bottom-hole pressure of 8 MPa to continue production. We define the time when the CO_2 mass fraction in the gas produced by the production well exceeds 20% as the CO_2 breakthrough time, because at this time the well will be shut down due to the high cost of natural gas separation. The detailed parameters of the numerical simulation model are shown in Table 1. During the numerical simulation process, the production dynamics of the CO_2 flooding process are evaluated by monitoring the following parameters: (1) spatial distribution of reservoir pressure and CO_2 mass fraction, (2) CH_4 and CO_2 mass rates in the production well, (3) CH_4 recovery, and (4) the amount of supercritical CO_2 stored in the pores and dissolved CO_2 in the formation water.

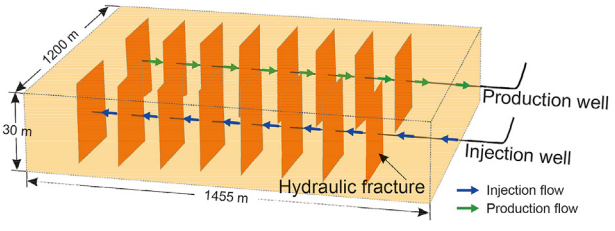

Fig. 1. Schematic diagram of CO_2 flooding model for multi-stage fracturing horizontal wells in tight gas reservoirs.

4. Results and discussion

4.1. Production performance under different CO_2 injection rates

4.1.1. Dynamic behavior of gas production and CO_2 sequestration

Fig. 2 shows the evolution of mass rates of CH_4 and CO_2 components at different injection rates. It can be seen that CH_4 is produced in the production well in a short period of time after CO_2 injection, which mainly comes from the free gas in the hydraulic fracture. As the gas in the hydraulic fracture is consumed, the CH_4 mass rate decreases rapidly. These characteristics are primarily associated with hydraulic fracturing and do not occur when the reservoir is not fractured (Luo et al., 2013). After CO_2 injection for about 80 d, the CH_4 mass rate is increased rapidly with time under the displacement pressure difference, confirming the feasibility of injecting CO_2 into depleted tight gas reservoirs to significantly increase gas production. In addition, the greater the injection rate, the higher the CH_4 mass rate, the earlier the CO_2 breakthrough in the production well, and the faster the CO_2 production rate increases. However, we find that as the injection rate increases, the magnitude of the CH_4 mass rate increase and the CO_2 breakthrough time decrease become smaller. Compared with the unfractured injection and production wells in tight gas reservoirs, the CH_4 production rate after hydraulic fracturing is significantly increased, which illustrates the superiority of multi-stage fracturing horizontal wells in implementing CO_2 flooding.

In order to evaluate the effect of the cumulative CO_2 injection amount on CH_4 production, we plot the evolution of CH_4 recovery with injected hydrocarbon pore volume (HCPV) at different injection rates, as shown in Fig. 3. It can be seen that the CH_4 recovery increases slowly with HCPV after the injection starts, indicating that the stimulation range in the early stage of CO_2 injection is mainly concentrated near the injection well and does not have a significant impact on natural gas production. As flooding proceeds, the stimulation range of CO_2 injection continues to expand, and the CH_4 recovery first increases rapidly and then increases approximately linearly with the injection process. At the end of production, the cumulative CO_2 injection amount of different schemes increases with the increase of injection rate. It is found that the HCPV when CO_2 breaks through is 0.38–0.50, while it is usually greater than 0.6 without fracturing (Liao et al., 2023). This indicates that CO_2 is more likely to break through after hydraulic fracturing, thereby reducing the cumulative injection amount of CO_2.

Fig. 4 compares CH_4 recovery and CO_2 storage amount at different injection rates at the end of production. We can see that the CH_4 recovery ranges from 20.0% to 23.8% under different injection rates, while the recovery without hydraulic fracturing is generally higher than 70%. As the CO_2 injection rate increases, the CH_4 recovery gradually decreases. This is mainly because increasing the injection rate significantly increases CH_4 production rate, but accelerates the breakthrough of CO_2 in the production well. It can also be found that as the injection rate increases, the amount of dissolved CO_2 in the formation water increases slightly, while the amount of supercritical CO_2 buried in the pores increases significantly. The above simulation results imply that the injection rate is one of the key engineering parameters that affects gas production and CO_2 storage efficiency of fracturing horizontal wells in tight gas reservoirs. Increasing the injection rate can indeed significantly increase the CH_4 production rate and CO_2 storage amount, but the CO_2 breakthrough is advanced, thereby reducing the CH_4 recovery. Moreover, an excessively high injection rate will rapidly increase the bottom hole pressure of the injection well, which may even lead to formation rock fracturing, thereby adversely affecting the production process. Therefore, it is recommended to optimize the injection rate by comprehensively considering factors such as CH_4

Table 1
Geological and engineering parameters of CO_2 flooding for numerical model (Fu et al., 2019; He et al., 2014; Ji et al., 2019; Wang et al., 2021; Wu et al., 2023; Zhao et al., 2024).

Parameter	Value	Parameter	Value
Reservoir thickness, m	30	Water salinity, mol/kg	0.812
Reservoir porosity	0.077	Diffusion coefficient in gaseous phase, m^2/s	1.6×10^{-7}
Horizontal permeability, $10^{-15}\mu m^2$	0.37	Diffusion coefficient in aqueous phase, m^2/s	8.0×10^{-9}
Vertical permeability, $10^{-15}\mu m^2$	0.037	Reservoir size in plane, m × m	1455 × 1200
Gas saturation	0.60	Horizontal well length, m	1065
Irreducible water saturation	0.40	Producer-injector spacing, m	615
Residual gas saturation	0.15	Bottom-hole pressure of producer, MPa	8.0
Rock compressibility, MPa^{-1}	5.0×10^{-5}	Number of hydraulic fractures	8
Initial reservoir pressure, MPa	25.0	Hydraulic fracture spacing, m	150
Reservoir temperature, °C	110	Half-length of hydraulic fractures, m	150
Water compressibility, MPa^{-1}	4.51×10^{-4}	Conductivity of hydraulic fractures, D·cm	40

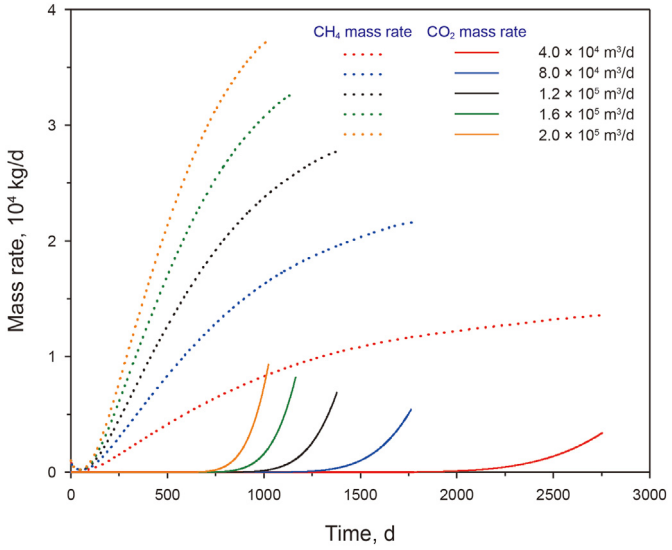

Fig. 2. Evolution of mass rates of CH_4 and CO_2 components under different injection rates.

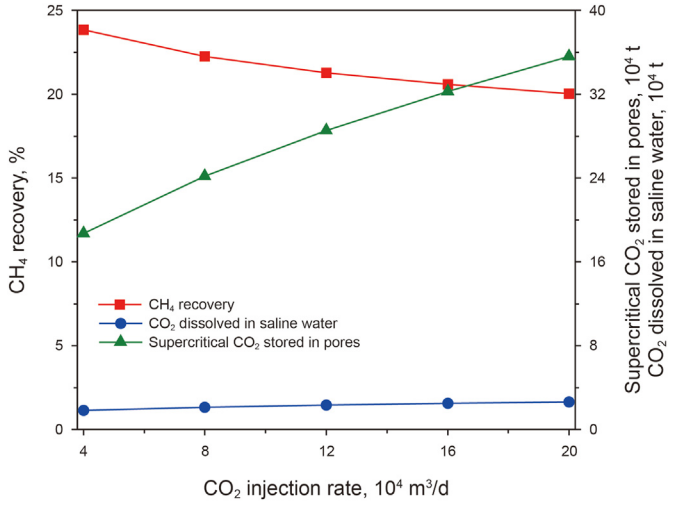

Fig. 4. Effect of injection rate on CH_4 recovery and CO_2 storage amount.

production efficiency, CO_2 storage amount, and the adverse effects of the project when implementing CO_2 enhanced gas recovery in field practice.

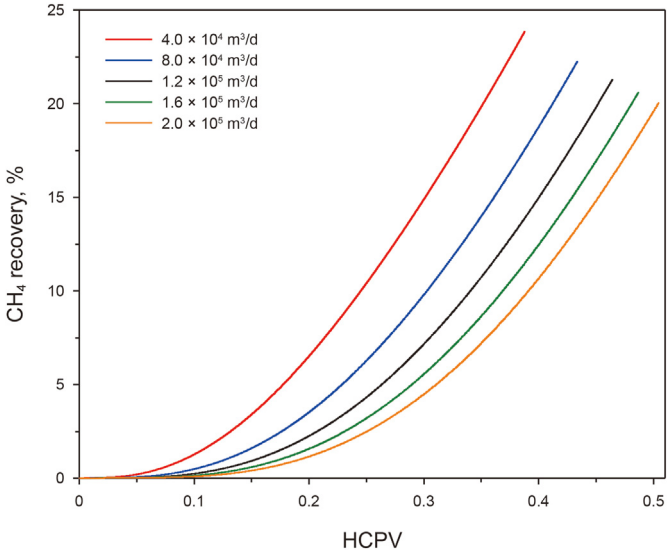

Fig. 3. Evolution of CH_4 recovery with HCPV under different injection rates.

4.1.2. Evolution characteristics of pressure and CO_2 spatial distribution

Fig. 5 shows the evolution of the pressure distribution over time on the horizontal plane with an injection rate of 1.2×10^5 m^3/d. It is noted that the horizontal plane locations of all physical parameter distributions involved in this work are located in the middle of the reservoir. At the beginning of production, the zone of increased pressure is mainly distributed near the hydraulic fractures of the injection well (Fig. 5(a)), and the corresponding gas production rate during this period is very low. As production proceeds, the zone of increased pressure expands along the injection well to the production well, and gas production rate begins to increase rapidly (Fig. 5(b)). Subsequently, the size of the zone of increased pressure between the injection well and the production well stabilizes, as the pressure near the injection well increases over time due to CO_2 injection (Fig. 5(c)–(f)). In this process, the gas production rate increases significantly with time until the CO_2 breakthrough in the production well. It can be seen that the reservoir pressure around the injection well is increased by 8.0–9.5 MPa at the end of production (Fig. 5(f)). Due to the low permeability of tight reservoirs, continued increase in CO_2 injection rate will significantly increase the bottom-hole pressure. A high production pressure difference can effectively increase gas production, but if the pressure is higher than the rock fracture pressure, it will cause formation fractures and adversely affect production.

Fig. 6 shows the evolution of CO_2 mass fraction distribution over time on the horizontal plane with an injection rate of 1.2×10^5 m^3/d. The distribution of CO_2 mass fraction is mainly controlled by flow

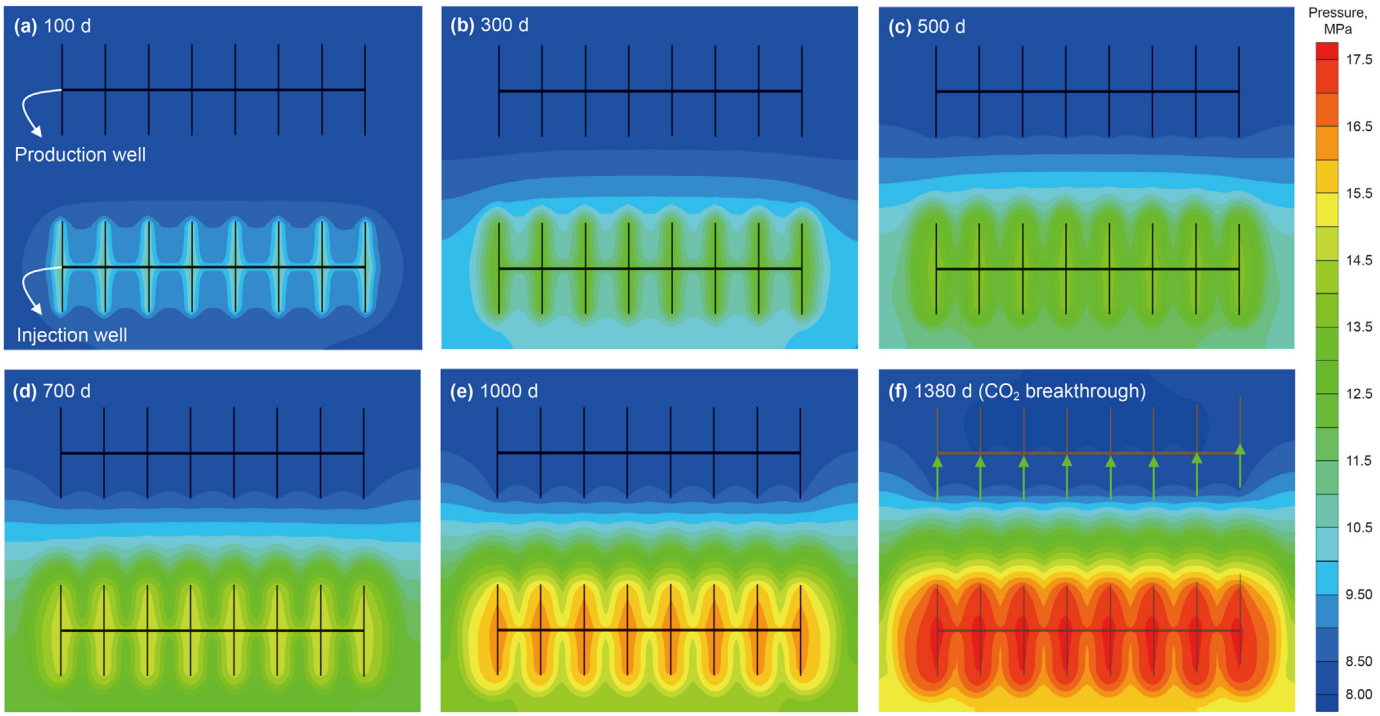

Fig. 5. Evolution of pressure distribution with time during CO_2 flooding.

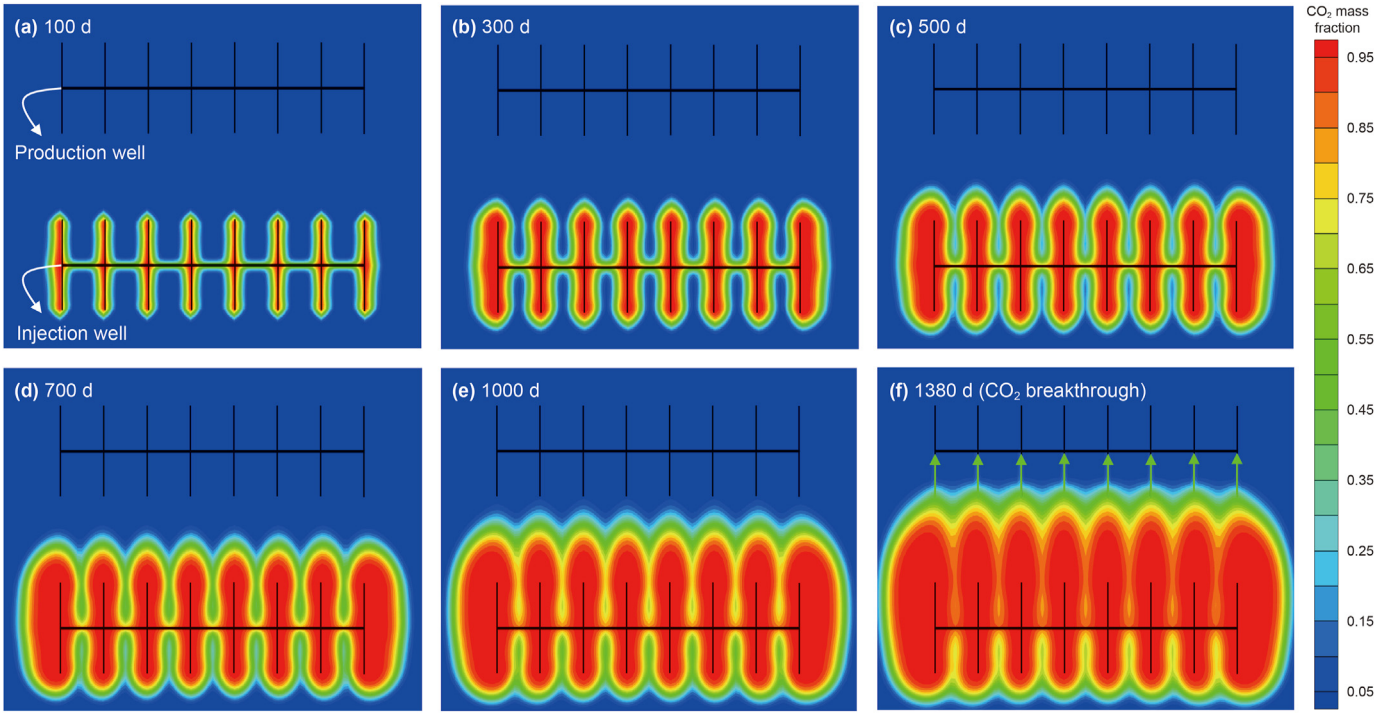

Fig. 6. Evolution of spatial distribution of CO_2 mass fraction over time during CO_2 flooding.

caused by pressure difference between wells and molecular diffusion caused by component concentration difference, among which hydraulic fractures significantly affect the distribution of pressure during flooding process. As can be seen from the figure, the CO_2 mass distribution can be divided into a CO_2 region (red region) due to fluid flow and a CO_2–CH_4 mixed area (green region) due to molecular diffusion. After production begins, CO_2 mainly flows from the injection well along the hydraulic fractures and diffuses along the fractures to the surrounding area (Fig. 6(a)), in which molecular diffusion plays an important role in the early stage of production. As production proceeds, CO_2 migrates laterally to the inter-fracture area and longitudinally along the hydraulic fractures

under the pressure difference, and the oval CO_2 zone and mixing zone around each fracture continue to expand (Fig. 6(b)–(d)). Subsequently, when the inter-fracture area is basically filled with CO_2, CO_2 mainly flows along the hydraulic fractures toward the production well (Fig. 6(e) and (f)). Once CO_2 flows into the hydraulic fracture of production well, it will flow along the fracture, causing a rapid breakthrough of CO_2. In addition, affected by the flow interference between fractures, the sweep efficiency of the region around the hydraulic fractures at both ends of the horizontal well is higher. It can be concluded that hydraulic fracturing can significantly reduce flow resistance and promote production in tight gas reservoirs, but it also accelerates CO_2 breakthrough along hydraulic fractures, resulting in a large amount of CH_4 remaining around the production well, thereby reducing sweep efficiency and CH_4 recovery.

4.2. Effect of hydraulic fracture parameters on enhanced gas recovery and CO_2 storage

The above simulation results imply that fractures generated by hydraulic fracturing of horizontal wells in tight gas reservoirs can change the flow field distribution, thereby having a significant impact on gas production and CO_2 breakthrough. Therefore, in this section, the impact of hydraulic fracture parameters on production dynamics is discussed, including hydraulic fracture distribution, number of hydraulic fractures, perforation position of the injection and production well, stimulated reservoir volume, fracture conductivity, and fracture half-length.

4.2.1. The influence of hydraulic fracture distribution

When deploying multi-stage fracturing schemes in tight gas reservoirs, the layout of hydraulic fractures will be optimized to achieve optimal development results. With the same average fracture half-length, the production dynamics under five types of hydraulic fracture distribution that may be involved in the development of tight gas reservoirs are simulated, as shown by the black solid line in Fig. 7. In the basic scheme, the half-length of hydraulic fractures is 150 m. In schemes 1 and 2, the half-length of the fracture linearly decreases or increases linearly from the center of the horizontal well to both ends, with the shortest half-length of the fracture being 90 m and the longest being 210 m. The difference is that in scheme 1, long fractures and short fractures are distributed oppositely, while in scheme 2, long hydraulic fractures and short fractures are single well staggered. In schemes 3 and 4, long fractures with a half-length of 210 m and short fractures with a half-length of 90 m are inter-well staggered, and the difference lies in the order in which the long and short fractures are deployed along the horizontal well.

It can be seen from the comparison pictures that under the same half-length fracture scheme, CO_2 flows uniformly from the injection well to the production well along the hydraulic fractures. For scheme 1, the distance between the hydraulic fractures at both ends of the injection well and the production well is the shortest, while the distance between the fractures at the center is the longest. Therefore, CO_2 preferentially flows to the production well along the hydraulic fractures at both ends of the horizontal well and breaks through. Compared with other schemes, there is a large amount of CH_4 remaining in the inter well area in the middle of the horizontal well after CO_2 breakthrough. For schemes 2–4, long fractures and short fractures are staggered, which results in a long longitudinal flow distance of CO_2 at long fracture locations in the injection well, while a short longitudinal flow distance of CO_2 at short fracture locations. It can be seen that the sweep efficiency in the area around long fractures is the highest during CO_2 breakthrough, while the sweep efficiency in the area around short fractures is the lowest. Therefore, although there are differences in the sweep areas between the three schemes and scheme 1, the sweep efficiency within the gas reservoir will be similar to scheme 1.

Fig. 8 compares the effects of hydraulic fracture distribution on the mass rates of CH_4 and CO_2 components. It can be seen that the

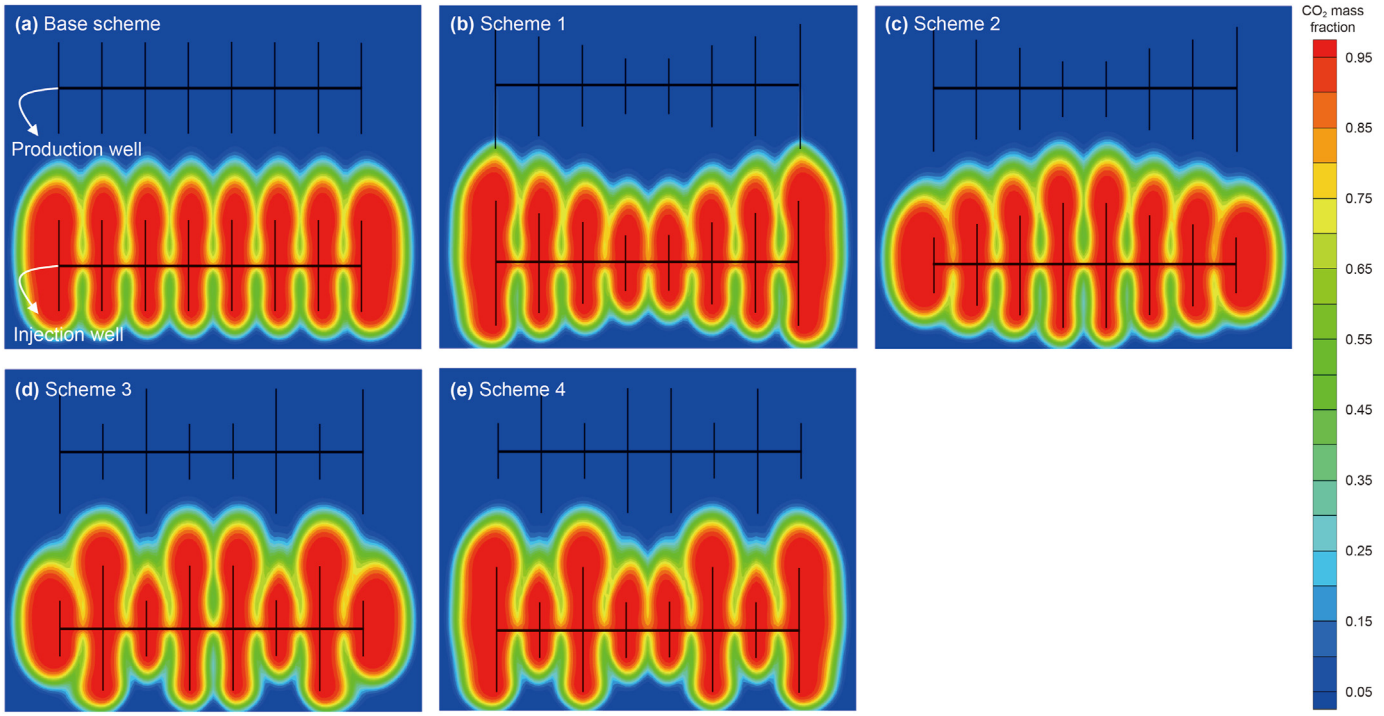

Fig. 7. Comparison of spatial distribution of CO_2 mass fraction under different hydraulic fracture deployments (at time 900 d).

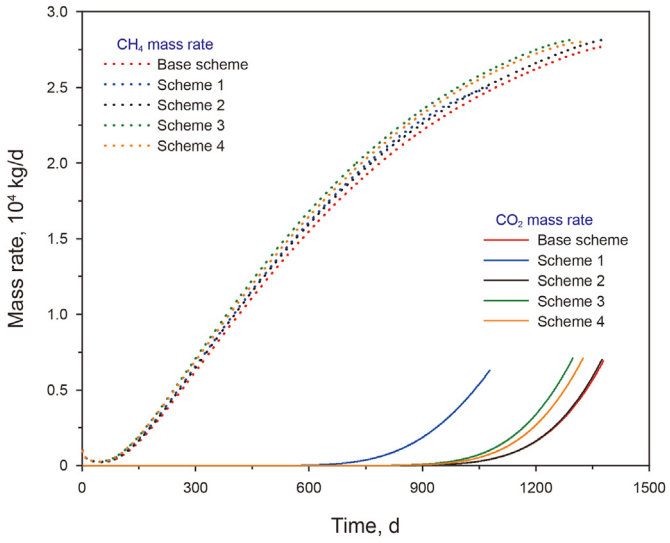

Fig. 8. Effect of hydraulic fracture distribution on mass rates of CH_4 and CO_2 components.

hydraulic fracture distribution has a significant impact on the CO_2 breakthrough time, but has a small impact on the CH_4 mass rate. The CH_4 mass rates in schemes 1 and 2 are basically the same, and their values are slightly higher than those in the basic scheme. While in scheme 1, since the fluid easily flows into the production well at the end of the horizontal well, the CO_2 breakthrough time is significantly reduced, which is 301 d shorter than the basic scheme. In contrast, the CH_4 mass rate in schemes 3 and 4 is higher, and the CO_2 breakthrough time is shortened by 54–81 d compared with the basic scheme.

Fig. 9 compares the CH_4 recovery and CO_2 storage amount under different hydraulic fracture deployments. It can be seen that the CH_4 recovery and CO_2 storage amount under different schemes are consistent. Since the CO_2 breakthrough time in scheme 1 is the shortest, the CH_4 recovery and CO_2 storage amount are the smallest, and its recovery is 34.1% lower than the basic scheme. In scheme 2, the CH_4 recovery and CO_2 storage amount are the largest, and its recovery increases by 0.4% compared with the basic scheme. In

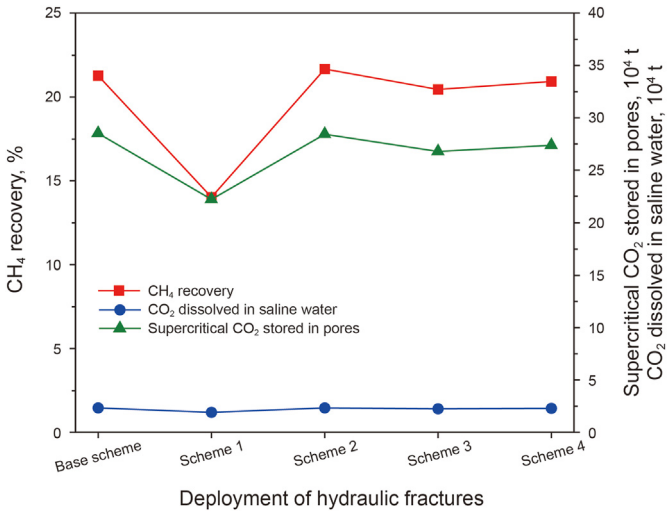

Fig. 9. Effect of hydraulic fracture distribution on CH_4 recovery and CO_2 storage amount.

contrast, the CH_4 recovery and CO_2 storage amount of schemes 3 and 4 are slightly lower than those of the basic scheme. Therefore, when CO_2 is injected into tight gas reservoirs to increase recovery under multi-stage fracturing horizontal wells, the production efficiency is lowest when long fractures and short fractures are distributed correspondingly at the location of the injection and production wells. In order to obtain better production results, it is recommended that each hydraulic fracture has a uniform length, or that long hydraulic fractures or short fractures are staggered.

4.2.2. The influence of number of hydraulic fractures

To investigate the effect of the number of hydraulic fractures (fracture spacing) on the CO_2 flooding efficiency of tight gas reservoirs, the production dynamics are simulated when the number of fractures was 4, 6, 8, 10, and 12, while other fracture parameters remained unchanged. Fig. 10 compares the spatial distribution of CO_2 mass fraction under different numbers of fractures when the flooding time is 900 d.

Since the total CO_2 injection amount of the injection well is the same, the greater the number of hydraulic fractures, the less CO_2 injection amount allocated to each fracture. Therefore, it can be seen that the swept area around each hydraulic fracture decreases as the number of fractures increases. From the perspective of the flooding characteristics of the gas reservoir, when the number of hydraulic fractures is less than 8, as the number of fractures increases, the swept area around the injection well gradually increases, which implies that the CO_2 injection flooding effect continues to strengthen. However, when the number of hydraulic fractures is greater than 8, it is found that CH_4 in the area around the injection well is basically affected, resulting in the flooding effect not changing with the increase of the number of fractures.

Fig. 11 shows the effect of the number of hydraulic fractures on the mass rates of CH_4 and CO_2 components. It can be seen that when the number of hydraulic fractures is less than 8, the CH_4 mass rate continues to increase as the number of fractures increases. When the number of fractures is greater than 8, the increase in CH_4 mass rate slightly changes with the increase in the number of fractures. In addition, the time when production wells start producing CO_2 is the same for different numbers of fractures, while the CO_2 breakthrough time decreases with the increase of the number of fractures.

Fig. 12 shows the effect of the number of hydraulic fractures on CH_4 recovery and CO_2 storage amount at the end of production. We see that as the number of fractures increases from 4 to 8, the CH_4 recovery increases by 2.3%, while when the number of fractures is greater than 8, the CH_4 recovery remains basically unchanged with the increase of the number of fractures. The change in CO_2 storage implies that as the number of fractures increases, the amount of supercritical CO_2 stored in the pores decreases slightly, while the amount of dissolved CO_2 in the formation water remains unchanged. Therefore, under these geological and engineering parameter conditions, the optimal number of fractures for CO_2 flooding in the tight gas reservoir in this study is 8. It should be noted that CO_2 flooding is usually implemented under the existing well pattern of depleted tight gas reservoirs, so the number of fractures is mainly determined during the initial fracturing construction of the gas reservoir. Therefore, the above research results will contribute to a deeper understanding of the impact of fracture parameters on the production performance of CO_2 flooding.

4.2.3. The influence of hydraulic fracture half-length

During the depressurization development process in tight gas reservoirs, increasing the length of hydraulic fractures can more effectively improve the flow capacity of the reservoir and increase gas production. However, for CO_2 flooding in depleted gas

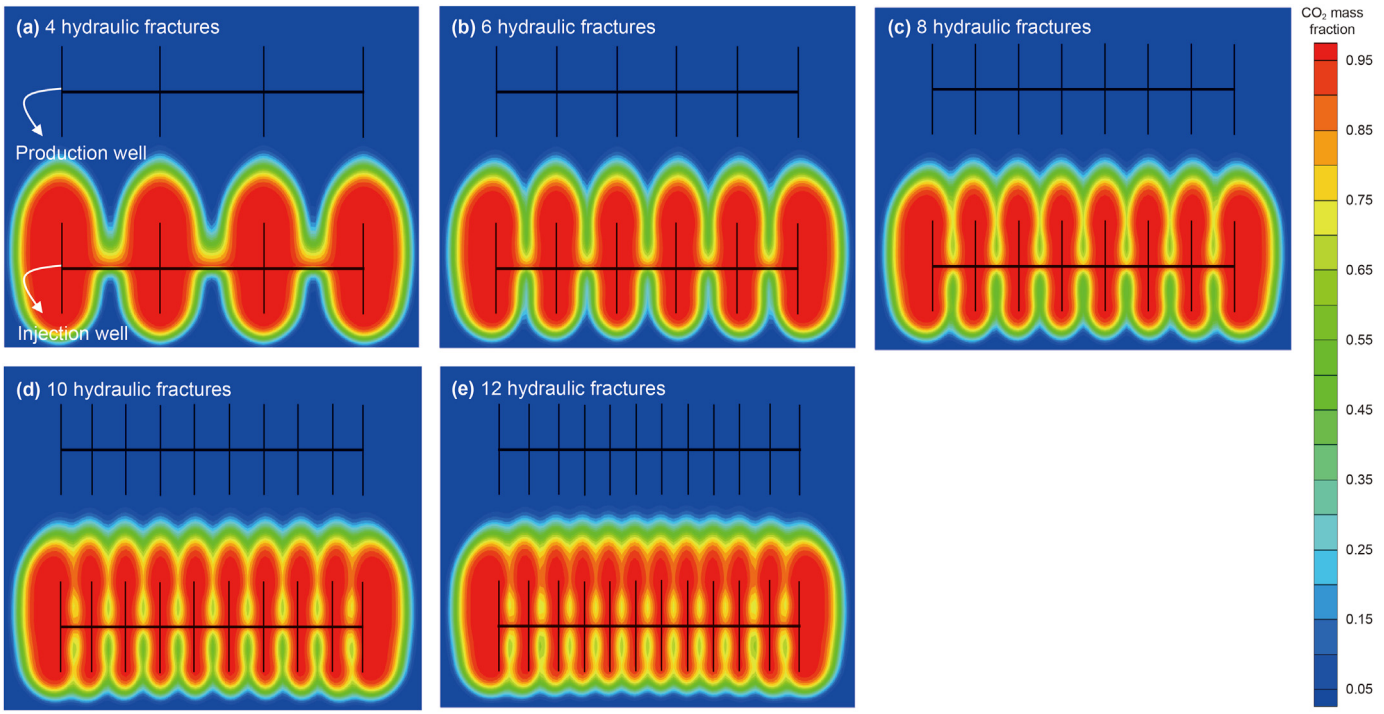

Fig. 10. Comparison of spatial distribution of CO_2 mass fraction under different numbers of fractures (at time 900 d).

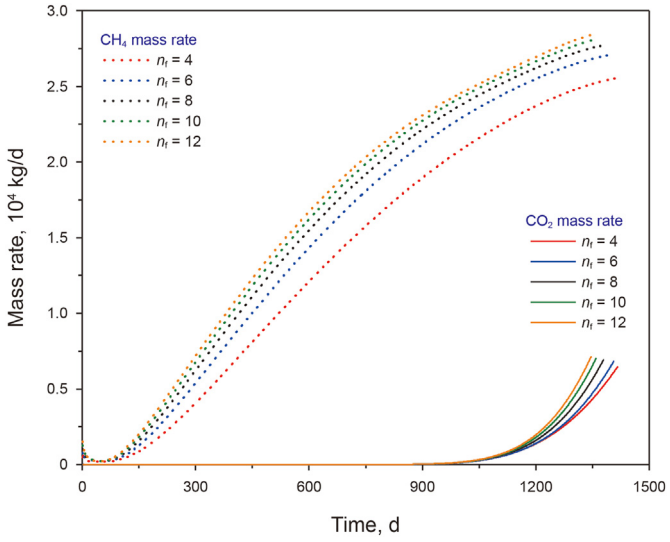

Fig. 11. Effect of the number of hydraulic fractures on mass rates of CH_4 and CO_2 components.

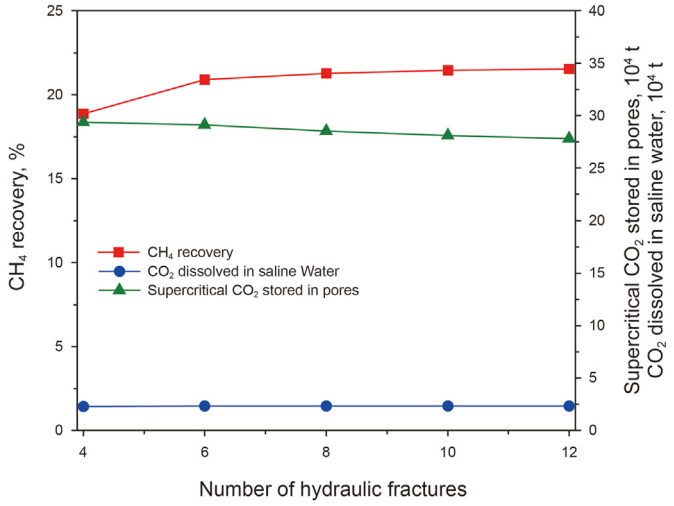

Fig. 12. Effect of the number of hydraulic fractures on CH_4 recovery and CO_2 storage amount.

reservoirs, increasing the fracture length will not only increase CH_4 production, but also have an important impact on CO_2 storage. Fig. 13 shows the effect of the hydraulic fracture half-length on the CH_4 and CO_2 mass rates, where the fracture half-length is set to 90, 120, 150, 180, and 210 m, respectively. As the fracture half-length increases, the contact area between the hydraulic fracture surface and the reservoir increases, thereby significantly increasing the CH_4 mass rate. It can also be seen that increasing the fracture half-length accelerates the CO_2 breakthrough in the production well, and the trends of the CO_2 mass rate curves under different fracture half-lengths are basically the same.

Fig. 14 shows the effect of hydraulic fracture half-length on CH_4 recovery and CO_2 storage amount at the end of production. It can be seen that the CH_4 recovery and the amount of supercritical CO_2 stored in the pores decrease linearly with the increase of the fracture half-length. As the half-length of the hydraulic fracture increases from 90 to 210 m, the CH_4 recovery and the amount of supercritical CO_2 stored decrease by 55.4% and 50.1%, respectively. In addition, the amount of dissolved CO_2 in formation water decreases with the increase of fracture half-length, but the proportion of dissolved CO_2 to the total CO_2 storage is low under different fracture half lengths. The above results imply that the long hydraulic fractures desired during fracturing of tight gas reservoirs can increase the gas production rate and recovery during the depletion development stage, but this will accelerate CO_2

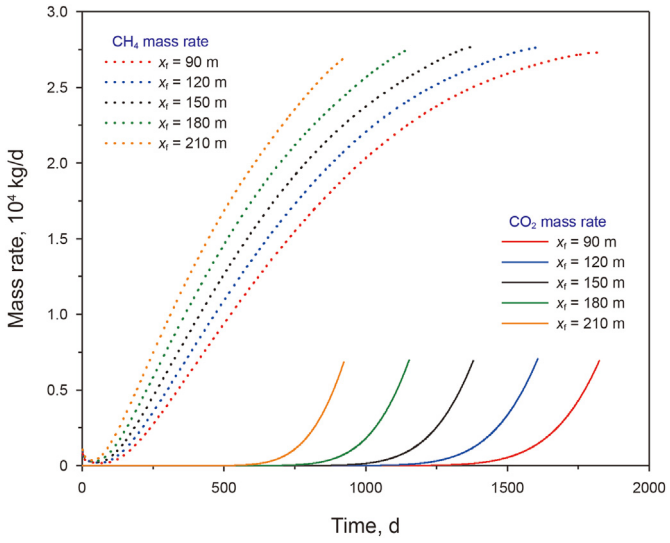

Fig. 13. Effect of hydraulic fracture half-length on mass rates of CH_4 and CO_2 components.

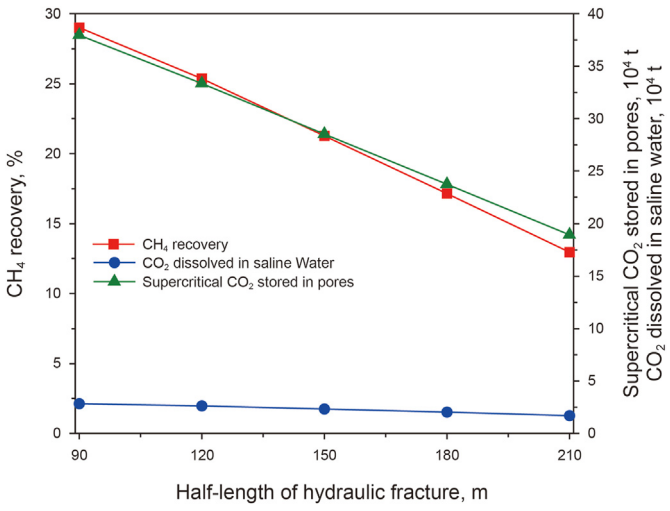

Fig. 14. Effect of hydraulic fracture half-length on CH_4 recovery and CO_2 storage amount.

breakthrough and lead to low CH_4 recovery during the CO_2 flooding stage. Therefore, reservoir blocks with small horizontal well spacing and long hydraulic fractures in tight gas reservoirs are not the optimal target areas for implementing CO_2 flooding to enhance gas recovery and CO_2 storage engineering.

4.2.4. The influence of hydraulic fracture conductivity

Hydraulic fracture conductivity is one of the important parameters to optimize during fracturing construction, which is defined as the product of the hydraulic fracture permeability and the fracture width. It represents the ability of a hydraulic fracture to allow fluid to pass through, and is related to factors such as the mechanical properties of the rock, closure pressure, reservoir damage, physical properties of the proppant, and paving concentration (Fan et al., 2019; Wang and Elsworth, 2018; Wu et al., 2022). Fig. 15 shows the effect of hydraulic fracture conductivity on the mass rates of CH_4 and CO_2 components, where the conductivity is set to 20, 40, 60, 80, and 100 D·cm, respectively. It can be seen that when the fracture conductivity is less than 40 D·cm, increasing the

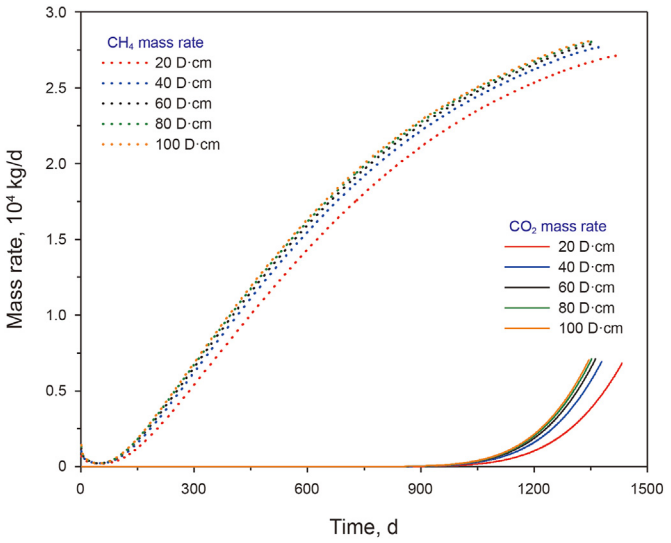

Fig. 15. Effect of hydraulic fracture conductivity on mass rates of CH_4 and CO_2 components.

conductivity can increase the CH_4 mass rate and advance the CO_2 breakthrough, but the impact of the conductivity on the CO_2 flooding process is limited. When the fracture conductivity is greater than 40 D·cm, the effect of conductivity on the mass rates of CH_4 and CO_2 components can be ignored. This is mainly because the flow capacity of the fractures to the production well is sufficient to meet production requirements, but the flow capacity of the reservoir to the fractures is insufficient.

Fig. 16 shows the effect of hydraulic fracture conductivity on CH_4 recovery and CO_2 storage amount. It can be seen that when the fracture conductivity increases from 20 to 40 D·cm, the CH_4 recovery and the amount of supercritical CO_2 stored in the pores decrease by 1.2% and 3.9%. When the fracture conductivity is greater than 40 D·cm, the CH_4 recovery and the amount of supercritical CO_2 stored are basically not affected by the conductivity. Therefore, the effect of fracture conductivity on CH_4 recovery and CO_2 storage can be basically ignored. During the depletion development process of tight gas reservoirs, fracture conductivity usually decreases to a certain extent over time due to factors such as

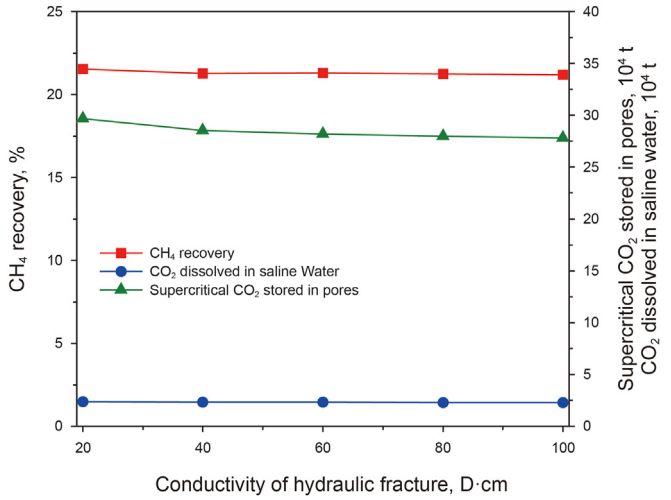

Fig. 16. Effect of hydraulic fracture conductivity on CH_4 recovery and CO_2 storage amount.

drop in reservoir pressure, reservoir damage, proppant fragmentation and migration. Therefore, re-fracturing technology is usually employed to increase production (Artun and Kulga, 2020). The simulation results of this work imply that when the fracture conductivity remains above 20 D·cm, it is not necessary to enhance the fracture conductivity through re-fracturing.

4.2.5. The influence of perforation location of hydraulic fractures

In the depletion development stage of tight gas reservoirs, perforation is usually performed in each hydraulic fracture to obtain high gas production rate and gas recovery. In order to improve the sweep efficiency of CO_2 flooding in depleted gas reservoirs, the perforations of corresponding hydraulic fractures in injection and production wells can be artificially blocked, thereby changing the direction of fluid flow. In addition to the basic scheme, four additional perforation schemes are considered, and the number of fractures perforated in injection wells and horizontal wells in each scheme is set to 4, as shown in Fig. 17. The black triangle symbols in the figure represent perforations in the corresponding hydraulic fractures, and the white dotted lines indicate the direction of CO_2 flow from the injection well to the production well.

The perforations of injection wells and production wells in schemes 1 and 2 are staggered. The difference is that in scheme 1, the hydraulic fractures at both ends of the injection well are perforated, while in scheme 2, the perforations of the hydraulic fractures at both ends of the injection well are blocked. In scheme 3, four fractures are perforated at both ends of the injection well and four fractures are perforated in the center of the production well. In scheme 4, the four fractures in the center of the injection well are perforated, and the four fractures at both ends of the production well are perforated. It can be seen that due to the staggered distribution of perforations in schemes 1 and 2, CO_2 flows in the lateral and diagonal directions from the hydraulic fractures of the injection well during the flooding process. As a result, these two schemes delay the CO_2 breakthrough and increase the sweep efficiency compared with the base scheme (Fig. 17(b) and (c)). In schemes 3 and 4, CO_2 flows diagonally from the hydraulic fracture in the injection well into the production well, thereby delaying CO_2 breakthrough. However, due to multiple consecutive hydraulic fractures not being perforated, a large amount of CH_4 has not been displaced in the center or at both ends of the injection well (Fig. 17(d) and (e)).

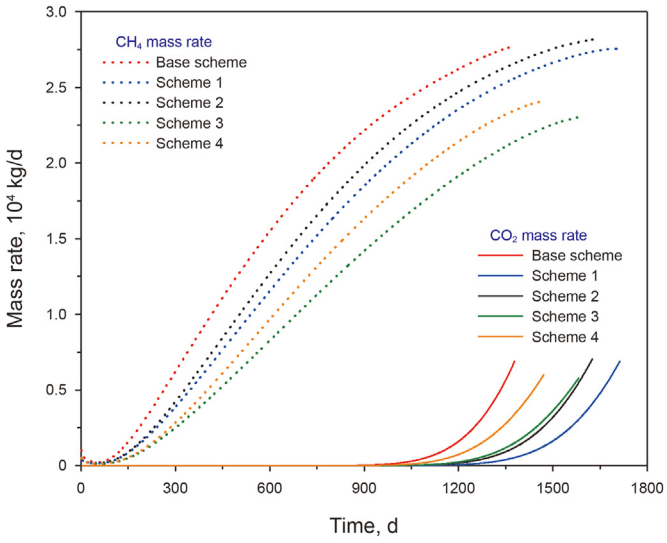

Fig. 18. Effect of perforation position of hydraulic fractures on mass rates of CH_4 and CO_2 components.

Fig. 18 shows the effect of the perforation position of hydraulic fractures on the mass rate of CH_4 and CO_2 components. It can be seen that in the base scheme, all the hydraulic fractures of the injection and production wells are perforated, resulting in the highest CH_4 mass rate, but the earliest breakthrough of CO_2. In schemes 1 and 2, the staggered and spaced perforation positions of injection wells and production wells improve the sweep efficiency, which

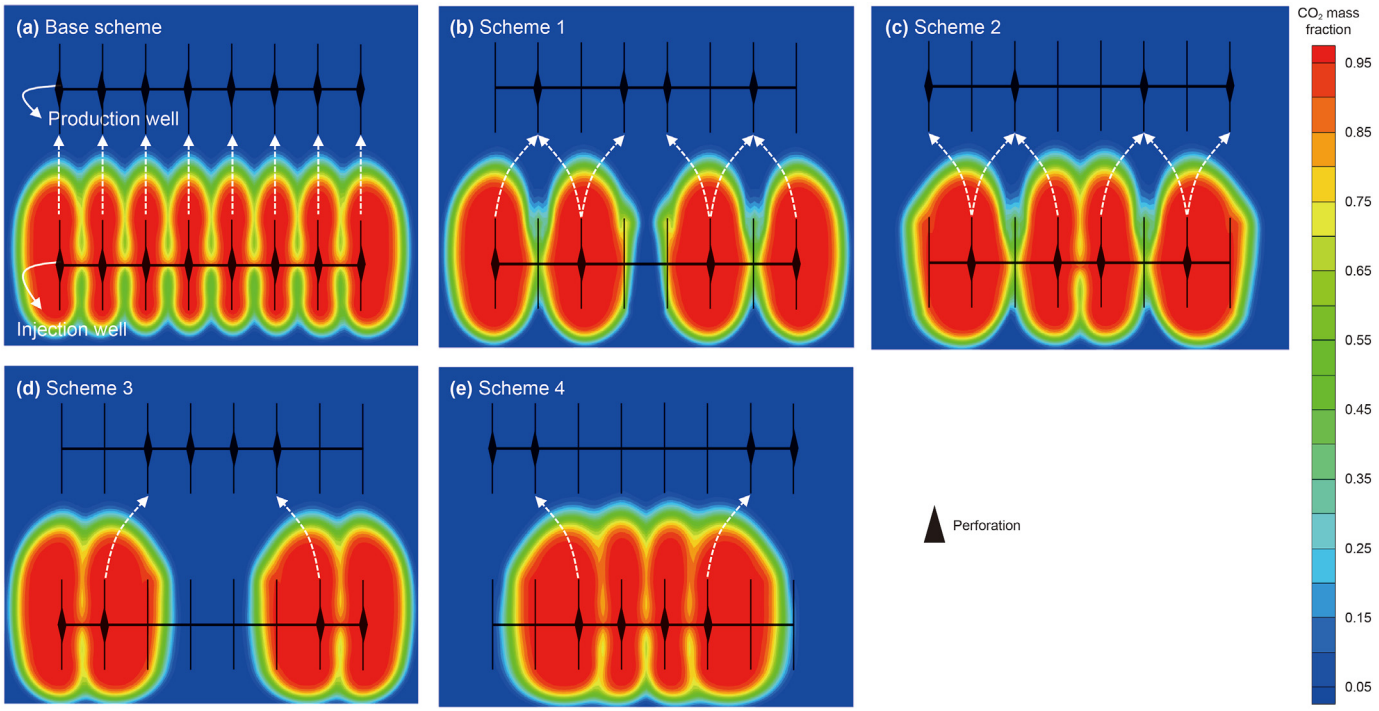

Fig. 17. Comparison of spatial distribution of CO_2 mass fraction under different fracture perforation schemes (at time 900 d).

results in a higher CH_4 mass rate than schemes 3 and 4, and CO_2 breakthrough is the latest.

Fig. 19 shows the effect of the perforation location of hydraulic fractures on CH_4 recovery and CO_2 storage amount. Among all the schemes, scheme 1 has the highest CH_4 recovery and CO_2 storage, with a 23.4% and 24.8% increase in CH_4 recovery and supercritical CO_2 sequestration in pores compared to the base scheme, respectively. In contrast, due to the low sweep efficiency of schemes 3 and 4, the CH_4 recovery is reduced by 15.6% and 17.6% respectively compared with the base scheme. However, the amount of supercritical CO_2 stored in the pores is increased by 15.4% and 7.4% respectively compared with the base scheme. In addition, the effect of perforation position of hydraulic fractures on dissolved CO_2 in formation water is negligible. Therefore, when implementing CO_2 flooding in depleted tight gas reservoirs, it is recommended that the hydraulic fractures of injection and production wells be perforated in staggered and spaced intervals to improve sweep efficiency, and thereby obtain higher gas recovery and CO_2 storage amount.

4.2.6. The influence of stimulated reservoir volume by massive hydraulic fracturing

In order to enhance the complexity of hydraulic fractures and generate a three-dimensional fracture network, massive hydraulic fracturing technology characterized by high pumping rate, high proppant concentration, and short fracturing spacing has been applied to the development of tight gas reservoirs in recent years (Lu et al., 2015; Umar et al., 2021). By changing the width of the fracturing stimulation zone, the influence of the stimulated reservoir volume (SRV) on gas production and CO_2 storage is studied. Fig. 20 compares the spatial distribution of CO_2 mass fraction under different SRVs. It can be seen that as the SRV increases, the flow resistance of CO_2 within the fracture network further decreases, thereby enhancing the displacement sweep efficiency in the inter-fracture area and slowing down the flow rate of CO_2 towards the production well.

Fig. 21 shows the effect of SRV on the mass rates of CH_4 and CO_2 components. The gas produced at the beginning of production mainly comes from hydraulic fractures, and the amount of this gas is limited. Therefore, SRV does not show a significant impact on the CH_4 mass rate in the early stages of production. After about 150 d of production, the flow of gas in the reservoir matrix to the hydraulic fracture network begins to become apparent. A larger SRV means lower flow resistance in the zone around the production well, resulting in a higher CH_4 mass rate. In the later stages of production, the CH_4 mass rates under different SRV conditions tend to be the same. In addition, as SRV increases, the lateral sweep efficiency of CO_2 in the zone around the injection well increases, thereby delaying CO_2 breakthrough.

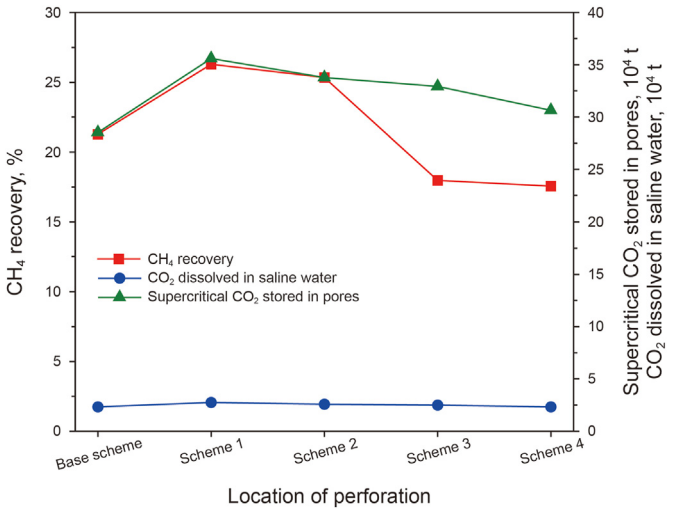

Fig. 19. Effect of perforation position of hydraulic fractures on CH_4 recovery and CO_2 storage amount.

Fig. 22 shows the effect of SRV on CH_4 recovery and CO_2 storage amount at the end of production. As SRV increases, the CH_4 recovery and the amount of supercritical CO_2 stored in the pores increase approximately linearly, while the amount of dissolved CO_2 in the formation water is generally not affected by SRV. We can see that when the SRV increases from 3.12×10^6 to 9.07×10^6 m^3, the CH_4 recovery and supercritical CO_2 storage amount is increased by 28.8% and 11.2%, respectively. This is mainly attributed to the fact that increasing the SRV size delays the CO_2 breakthrough while increasing the mass rate of CH_4. Therefore, it can be concluded that horizontal wells with complex fracture networks can achieve more favorable production efficiency when implementing CO_2 flooding projects.

5. Conclusions

In this work, the production behavior of CO_2 flooding with multi-stage fracturing horizontal wells in depleted tight sandstone gas reservoirs is studied through numerical simulation method. The dynamic characteristics of enhanced gas recovery and CO_2 storage are analyzed, and the influence of hydraulic fracture parameters on production performance is examined. The following conclusions can be drawn:

(1) Due to the dual effects of low flow resistance in hydraulic fractures and pressure supplementation by CO_2 injection, the production rate of multi-stage fracturing horizontal wells is significantly increased after CO_2 flooding. Compared with unfractured tight gas reservoirs, the CH_4 production rate is significantly higher, but CO_2 flow along fractures accelerates CO_2 breakthrough, resulting in lower CH_4 recovery and cumulative CO_2 injection.

(2) Increasing the CO_2 injection rate can significantly increase the CH_4 production and CO_2 storage amount, but it will advance the CO_2 breakthrough, thus reducing the CH_4 recovery. Moreover, the excessively high injection rate causes a rapid increase in the bottom-hole pressure, or even triggers formation fracturing. Therefore, it is recommended to fully consider factors such as CH_4 recovery, CO_2 storage amount, and adverse engineering effects to optimize the injection rate when implementing CO_2 flooding.

(3) As the number of hydraulic fractures increases, the sweep efficiency of CO_2 flooding in the zone around the injection well increases, thereby increasing the CH_4 mass rate and recovery. However, when the number of fractures is more than 8, the impact on gas production and CO_2 storage is slight due to fracture interference.

(4) Increasing the length of hydraulic fractures can significantly increase the CH_4 mass rate, but accelerates CO_2 breakthrough, resulting in a linear decrease in CH_4 recovery and supercritical CO_2 storage. Therefore, gas reservoir blocks with small well spacing and long hydraulic fracture lengths are not priority for CO_2 flooding.

(5) Staggered and spaced perforations of fractures in injection wells and production wells can improve fluid flow paths, expand CO_2 sweep and delay CO_2 breakthrough, thereby increasing CH_4 recovery and CO_2 storage. The staggered distribution of long fractures and short fractures or uniform

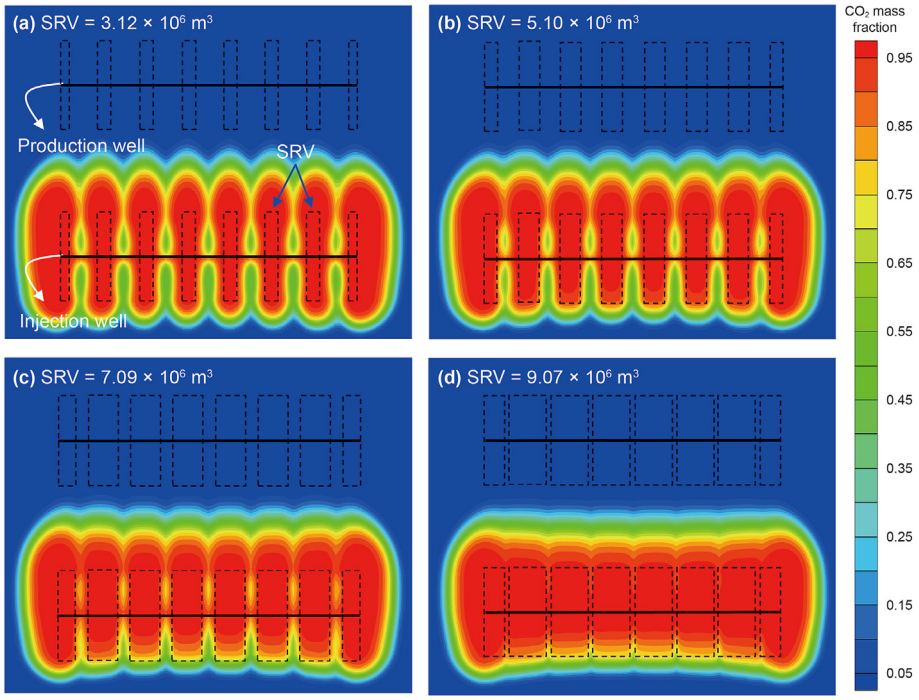

Fig. 20. Comparison of spatial distribution of CO_2 mass fraction under different SRVs (at time 900 d).

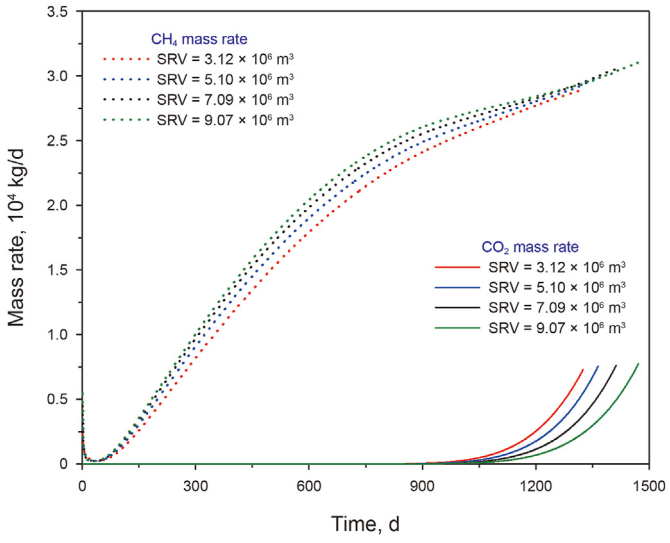

Fig. 21. Effect of stimulated reservoir volume on mass rates of CH_4 and CO_2 components.

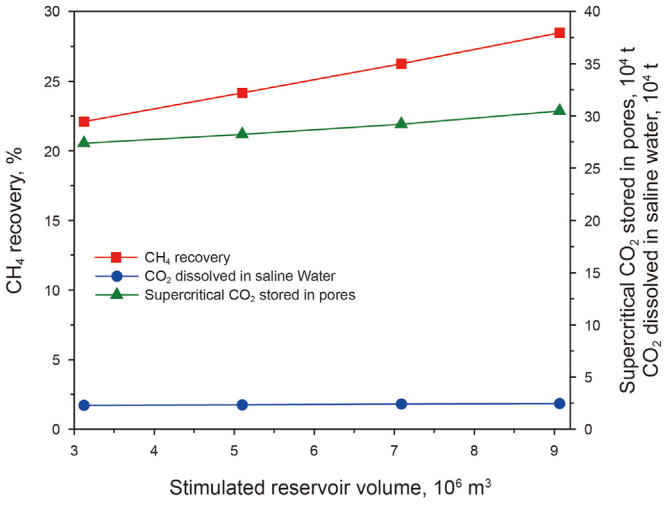

Fig. 22. Effect of stimulated reservoir volume on CH_4 recovery and CO_2 storage amount.

fracture length produces high production efficiency, while the opposite distribution of long fractures significantly accelerates CO_2 breakthrough, resulting in low flooding efficiency.

(6) The fracture network produced by massive hydraulic fracturing further reduces flow resistance and expands the flooding sweep in the inter-fracture zone. Increasing the SRV promotes CH_4 production and delays CO_2 breakthrough, resulting in CH_4 recovery and supercritical CO_2 storage amount increasing linearly with the SRV.

Tight sandstone gas reservoirs are characterized by low porosity and extremely low permeability. During CO_2 flooding, CO_2 may preferentially adsorb on the rock surface to replace the adsorbed CH_4, thereby increasing the CH_4 recovery and CO_2 sequestration. Previous research results have shown that the adsorption mode of gas in tight sandstone is mainly filled with slit pore structure, and the adsorption capacity is much lower than that of shale and coal seam, and the CO_2 flooding process is less affected by competitive adsorption (Zhang et al., 2025). On the other hand, experimental studies on CO_2-CH_4 competitive adsorption in tight sandstone gas reservoirs are scarce, resulting in the lack of accurate parameters for the simulation of competitive adsorption behavior in numerical simulation models. In the future work, it is important to perform CO_2-CH_4 competitive adsorption experiments of tight sandstone gas reservoirs, and establish a competitive adsorption characterization model.

CRediT authorship contribution statement

Er-Meng Zhao: Writing – original draft, Visualization, Methodology, Investigation, Formal analysis, Conceptualization. **Zhi-Jun Jin:** Supervision, Resources, Funding acquisition. **Gen-Sheng Li:** Supervision, Resources, Conceptualization. **Kai-Qiang Zhang:** Software, Investigation, Formal analysis. **Yue Zeng:** Investigation, Formal analysis.

Declaration of competing interest

The authors declare that they have no known competing financial interests or personal relationships that could have appeared to influence the work reported in this paper.

Acknowledgements

The authors appreciate the financial support of the National Natural Science Foundation of China (Grant No. 52304018) and China Postdoctoral Science Foundation (Grant No. 2023TQ0014, Grant No. 2023M730088).

References

Artun, E., Kulga, B., 2020. Selection of candidate wells for re-fracturing in tight gas sand reservoirs using fuzzy inference. Petrol. Explor. Dev. 47 (2), 413–420. https://doi.org/10.1016/S1876-3804(20)60058-1.

Asif, M., Wang, L., Naveen, P., et al., 2024. Influence of competitive adsorption, diffusion, and dispersion of CH_4 and CO_2 gases during the CO_2-ECBM process. Fuel 358, 130065. https://doi.org/10.1016/j.fuel.2023.130065.

Bakker, R.J., 2003. Package FLUIDS 1. Computer programs for analysis of fluid inclusion data and for modelling bulk fluid properties. Chem. Geol. 194 (1–3), 3–23. https://doi.org/10.1016/S0009-2541(02)00268-1.

Blasingame, T.A., 2008. The characteristic flow behavior of low-permeability reservoir systems. In: SPE Unconventional Resources Conference/Gas Technology Symposium. https://doi.org/10.2118/114168-MS.

Davoodi, S., Al-Shargabi, M., Wood, D.A., et al., 2023. Review of technological progress in carbon dioxide capture, storage, and utilization. Gas Science and Engineering 205070. https://doi.org/10.1016/j.jgsce.2023.205070.

Ding, J., Yan, C., He, Y., et al., 2021. Supercritical CO_2 sequestration and enhanced gas recovery in tight gas reservoirs: feasibility and factors that influence efficiency. Int. J. Greenh. Gas Control 105, 103234. https://doi.org/10.1016/j.ijggc.2020.103234.

Ding, J., Yan, C., Wang, G., et al., 2022. Competitive adsorption between CO_2 and CH_4 in tight sandstone and its influence on CO_2-injection enhanced gas recovery (EGR). Int. J. Greenh. Gas Control 113, 103530. https://doi.org/10.1016/j.ijggc.2021.103530.

Edouard, M.N., Okere, C.J., Ejike, C., et al., 2023. Comparative numerical study on the co-optimization of CO_2 storage and utilization in EOR, EGR, and EWR: Implications for CCUS project development. Appl. Energy 347, 121448. https://doi.org/10.1016/j.apenergy.2023.121448.

Ennis-King, J., Dance, T., Xu, J., et al., 2011. The role of heterogeneity in CO_2 storage in a depleted gas field: History matching of simulation models to field data for the CO2CRC Otway Project, Australia. Energy Proc. 4, 3494–3501. https://doi.org/10.1016/j.egypro.2011.02.276.

Fan, M., McClure, J., Han, Y., 2019. Using an experiment/simulation-integrated approach to investigate fracture-conductivity evolution and non-Darcy flow in a proppant-supported hydraulic fracture. SPE J. 24 (4), 1912–1928. https://doi.org/10.2118/195588-PA.

Fu, J., Fan, L., Liu, X., et al., 2019. Gas accumulation conditions and key exploration & development technologies in Sulige gas field. Acta Pet. Sin. 40 (2), 240–256. https://doi.org/10.7623/syxb201902013 (in Chinese).

Gao, X., Yang, S., Tian, L., et al., 2024. System and multi-physics coupling model of liquid-CO_2 injection on CO_2 storage with enhanced gas recovery (CSEGR) framework. Energy 130951. https://doi.org/10.1016/j.energy.2024.130951.

Garcia, J.E., 2001. Density of Aqueous Solutions of CO_2. Lawrence Berkeley National Lab. https://doi.org/10.2172/790022.

Guo, Z., Jia, A., Ji, G., 2017. Reserve classification and well pattern infilling method of tight sandstone gasfield: A case study of Sulige gasfield. Acta Pet. Sin. 38 (11), 1299–1309. https://doi.org/10.7623/syxb201711009 (in Chinese).

Hamza, A., Hussein, I.A., Al-Marri, M.J., et al., 2021. CO_2 enhanced gas recovery and sequestration in depleted gas reservoirs: A review. J. Petrol. Sci. Eng. 196, 107685. https://doi.org/10.1016/j.petrol.2020.107685.

Harvey, A.H., 1996. Semiempirical correlation for Henry's constants over large temperature ranges. AIChE J. 42 (5), 1491–1494. https://doi.org/10.1002/aic.690420531.

He, C., Ji, Z., Geng, X., Zhou, M., 2023. The influence of irreducible water for enhancing CH_4 recovery in combination of CO_2 storage with CO_2 injection in gas reservoirs. Int. J. Greenh. Gas Control 126, 103919. https://doi.org/10.1016/j.ijggc.2023.103919.

He, M., Ma, X., Zhang, Y., 2014. A factory fracturing model of multi-well cluster in Sulige gas field, NW China. Petrol. Explor. Dev. 41 (3), 387–392. https://doi.org/10.1016/S1876-3804(14)60044-6.

He, Y., Liu, M., Tang, Y., et al., 2024. CO_2 storage capacity estimation by considering CO_2 dissolution: A case study in a depleted gas Reservoir, China. J. Hydrol. 630, 130715. https://doi.org/10.1016/j.jhydrol.2024.130715.

Ji, G., Jia, A., Meng, D., et al., 2019. Technical strategies for effective development and gas recovery enhancement of a large tight gas field: A case study of Sulige gas field, Ordos Basin, NW China. Petrol. Explor. Dev. 46 (3), 629–641. https://doi.org/10.1016/S1876-3804(19)60043-1.

Jia, Y., Shi, Y., Pan, W., et al., 2019. The feasibility appraisal for CO_2 enhanced gas recovery of tight gas reservoir: Experimental investigation and numerical model. Energies 12 (11), 2225. https://doi.org/10.3390/en12112225.

Jia, Y., Shi, Y., Yan, J., 2021. The feasibility appraisal for CO_2 enhanced gas recovery of tight gas reservoir: Case analysis and economic evaluation. In: International Petroleum Technology Conference. https://doi.org/10.2523/IPTC-21291-MS.

Li, M., Guo, Y., Li, Z., 2020. The diagenetic controls of the reservoir heterogeneity in the tight sand gas reservoirs of the Zizhou Area in China's east Ordos Basin: Implications for reservoir quality predictions. Mar. Petrol. Geol. 112, 104088. https://doi.org/10.1016/j.marpetgeo.2019.104088.

Li, S., Wang, P., Wang, Z., et al., 2023. Strategy to enhance geological CO_2 storage capacity in saline aquifer. Geophys. Res. Lett. 50 (3), e2022GL101431. https://doi.org/10.1029/2022GL101431.

Li, Z., Yu, H., Bai, Y., 2023. Numerical study on the influence of temperature on CO_2-ECBM. Fuel 348, 128613. https://doi.org/10.1016/j.fuel.2023.128613.

Liao, H., Pan, W., He, Y., et al., 2023. Study on the mechanism of CO_2 injection to improve tight sandstone gas recovery. Energy Rep. 9, 645–656. https://doi.org/10.1016/j.egyr.2022.11.210.

Liu, S., Ren, B., Li, H., et al., 2022a. CO_2 storage with enhanced gas recovery (CSEGR): A review of experimental and numerical studies. Petrol. Sci. 19 (2), 594–607. https://doi.org/10.1016/j.petsci.2021.12.009.

Liu, S., Yuan, L., Zhao, C., et al., 2022b. A review of research on the dispersion process and CO_2 enhanced natural gas recovery in depleted gas reservoir. J. Petrol. Sci. Eng. 208, 109682. https://doi.org/10.1016/j.petrol.2021.109682.

Lu, T., Liu, Y., Wu, L., 2015. Challenges to and countermeasures for the production stabilization of tight sandstone gas reservoirs of the Sulige Gasfield, Ordos Basin. Nat. Gas. Ind. B 2 (4), 323–333. https://doi.org/10.1016/j.ngib.2015.09.005.

Luo, F., Xu, R.N., Jiang, P.X., 2013. Numerical investigation of the influence of vertical permeability heterogeneity in stratified formation and of injection/production well perforation placement on CO_2 geological storage with enhanced CH_4 recovery. Appl. Energy 102, 1314–1323. https://doi.org/10.1016/j.apenergy.2012.07.008.

Luo, J., Xie, Y., Hou, M.Z., et al., 2023. Advances in subsea carbon dioxide utilization and storage. Energy Rev. 2 (1), 100016. https://doi.org/10.1016/j.enrev.2023.100016.

Meinshausen, M., Meinshausen, N., Hare, W., et al., 2009. Greenhouse-gas emission targets for limiting global warming to 2 °C. Nature 458 (7242), 1158–1162. https://doi:10.1038/nature08017.

Odi, U., 2012. Analysis and potential of CO_2 huff-n-puff for near wellbore condensate removal and enhanced gas recovery. In: SPE Annual Technical Conference and Exhibition. https://doi.org/10.2118/160917-STU.

Patel, M.J., May, E.F., Johns, M.L., 2017. Inclusion of connate water in enhanced gas recovery reservoir simulations. Energy 141, 757–769. https://doi.org/10.1016/j.energy.2017.09.074.

Prasad, S.K., Sangwai, J.S., Byun, H.S., 2023. A review of the supercritical CO_2 fluid applications for improved oil and gas production and associated carbon storage. J. CO_2 Util. 72, 102479. https://doi.org/10.1016/j.jcou.2023.102479.

Sambo, C., Liu, N., Shaibu, R., et al., 2023. A technical review of CO_2 for enhanced oil recovery in unconventional oil reservoirs. Geoenergy Science and Engineering 221, 111185. https://doi.org/10.1016/j.petrol.2022.111185.

Shen, W., Ma, T., Zuo, L., et al., 2024. Advances and prospects of supercritical CO_2 for shale gas extraction and geological sequestration in gas shale reservoirs. Energy Fuels 38 (2), 789–805. https://doi.org/10.1021/acs.energyfuels.3c03843.

Shi, Y., Jia, Y., Pan, W., 2017. Potential evaluation on CO_2-EGR in tight and low-permeability reservoirs. Nat. Gas. Ind. B 4 (4), 311–318. https://doi.org/10.1016/j.ngib.2017.08.013.

Singh, S., Boruah, A., Devaraju, J., 2023. CO_2 sequestration and CH_4 extraction from unmineable coal seams in Singrauli coalfield. International Journal of Coal Preparation and Utilization 1–18. https://doi.org/10.1080/19392699.2023.2280134.

Syah, R., Alizadeh, S.M., Nurgalieva, K.S., et al., 2021. A laboratory approach to measure enhanced gas recovery from a tight gas reservoir during supercritical carbon dioxide injection. Sustainability 13 (21), 11606. https://doi.org/10.3390/su132111606.

Tang, C., Zhou, W., Chen, Z., 2023. Numerical simulation of CO_2 sequestration in shale gas reservoirs at reservoir scale coupled with enhanced gas recovery. Energy 277, 127657. https://doi.org/10.1016/j.energy.2023.127657.

Umar, I.A., Negash, B.M., Quainoo, A.K., 2021. An outlook into recent advances on estimation of effective stimulated reservoir volume. J. Nat. Gas Sci. Eng. 88, 103822. https://doi.org/10.1016/j.jngse.2021.103822.

Underschultz, J., Boreham, C., Dance, T., et al., 2011. CO_2 storage in a depleted gas

field: an overview of the CO2CRC Otway Project and initial results. Int. J. Greenh. Gas Control 5 (4), 922–932. https://doi.org/10.1016/j.ijggc.2011.02.009.
Van der Meer, L.G.H., Kreft, E., Geel, C., et al., 2005. K12-B a test site for CO_2 storage and enhanced gas recovery. In: SPE Europec Featured at EAGE Conference and Exhibition.
Wang, F., Liu, Y., Hu, C., 2018. Experimental study on feasibility of enhanced gas recovery through CO_2 flooding in tight sandstone gas reservoirs. Processes 6 (11), 214. https://doi.org/10.3390/pr6110214.
Wang, J., Elsworth, D., 2018. Role of proppant distribution on the evolution of hydraulic fracture conductivity. J. Petrol. Sci. Eng. 166, 249–262. https://doi.org/10.1016/j.petrol.2018.03.040.
Wang, J., Zhang, C., Li, J., et al., 2021. Tight sandstone gas reservoirs in the Sulige Gas Field: development understandings and stable-production proposals. Nat. Gas. Ind. 41 (2), 100–110. https://doi.org/10.3787/j.issn.1000-0976.2021.02.012 (in Chinese).
Wang, W., Wen, J., Wang, C., et al., 2023. Current status and development trends of CO_2 storage with enhanced natural gas recovery (CS-EGR). Fuel 349, 128555. https://doi.org/10.1016/j.fuel.2023.128555.
Wang, Y.Y., Wang, X.G., Dong, R.C., et al., 2023. Reservoir heterogeneity controls of CO_2-EOR and storage potentials in residual oil zones: Insights from numerical simulations. Petrol. Sci. 20 (5), 2879–2891. https://doi.org/10.1016/j.petsci.2023.03.023.
Wu, Z., Cui, C., Jia, P., et al., 2022. Advances and challenges in hydraulic fracturing of tight reservoirs: A critical review. Energy Geosci. 3 (4), 427–435. https://doi.org/10.1016/j.engeos.2021.08.002.
Wu, Z., Jiang, Q., Zhou, Y., et al., 2023. Key technologies and orientation of EGR for the Sulige tight sandstone gas field in the Ordos Basin. Nat. Gas. Ind. B 10 (6), 591–601. https://doi.org/10.1016/j.ngib.2023.11.005.
Yoro, K.O., Daramola, M.O., 2020. CO_2 emission sources, greenhouse gases, and the global warming effect. In: Advances in Carbon Capture. Woodhead Publishing, pp. 3–28. https://doi.org/10.1016/B978-0-12-819657-1.00001-3.
Yu, H., Wang, Z., Li, J., 2023. Key technological progress and breakthrough direction for the development of complex tight gas reservoirs in Changqing gas field, Ordos Basin. Acta Pet. Sin. 44 (4), 698. https://doi.org/10.7623/syxb202304011 (in Chinese).
Zhang, C., Wang, E., Li, B., et al., 2023. Laboratory experiments of CO_2-enhanced coalbed methane recovery considering CO_2 sequestration in a coal seam. Energy 262, 125473. https://doi.org/10.1016/j.energy.2022.125473.
Zhang, K., Lau, H.C., Chen, Z., 2022. CO_2 enhanced gas recovery and sequestration as CO_2 hydrate in shallow gas fields in Alberta, Canada. J. Nat. Gas Sci. Eng. 103, 104654. https://doi.org/10.1016/j.jngse.2022.104654.
Zhang, L., Xiong, Y., Zhao, Y., et al., 2022. A reservoir drying method for enhancing recovery of tight gas. Petrol. Explor. Dev. 49 (1), 144–155. https://doi.org/10.1016/S1876-3804(22)60011-9.
Zhang, Y., Li, D., Xin, G., et al., 2025. An adsorption micro mechanism theoretical study of CO_2-rich industrial waste gas for enhanced unconventional natural gas recovery: comparison of coalbed methane, shale gas, and tight gas. Separ. Purif. Technol., 353, 128414. https://doi.org/10.1016/j.seppur.2024.128414.
Zhao, E., Jin, Z., Li, G., et al., 2024. Numerical simulation of CO_2 storage with enhanced gas recovery in depleted tight sandstone gas reservoirs. Fuel 371, 131948. https://doi.org/10.1016/j.fuel.2024.131948.
Zhao, J., Fu, J., Yao, J., et al., 2012. Quasi-continuous accumulation model of large tight sandstone gas field in Ordos Basin. Acta Pet. Sin. 33 (S1), 37–52. https://doi.org/10.7623/syxb2012S1006 (in Chinese).
Zuo, M., Chen, H., Qi, X., et al., 2023. Effects of CO_2 injection volume and formation of in-situ new phase on oil phase behavior during CO_2 injection for enhanced oil recovery (EOR) in tight oil reservoirs. Chem. Eng. J. 452, 139454. https://doi.org/10.1016/j.cej.2022.139454.